ISME

Uncertainty Analysis of Spray Injection Process in a Model Scale Liquid Fuel Micro-Motor

M. Nadjafi*
Assistance Professor

M.A. Farsi†
Associate Professor

F. Ommi‡
Professor

Injection process and its parameters are the most important factors in the combustion process that depends on some factors in operation. In this paper, initially, injection parameters from viewpoint of macroscopic and microscopic in a manufactured model scale liquid fuel micro-motor that are measured experimentally in Cold-Test and Phase Doppler Analyzer (PDA) laboratories, are evaluated. And then, Uncertainty Analysis (UA) methodologies for experimental uncertainty assessment are implemented to drive the respective block diagram. The sources of uncertainty associated with the techniques are presented, and where such data were available, quantitative estimates of their magnitude are given. Uncertainty analysis results that are taken to spraying parameters show the high accuracy of experimental test results. This framework is a comprehensive and complete technique that could be implemented and executed over any set to analyze uncertainty value, with difference that each set or case study has its respective parameters.

DOI: 10.30506/jmee.2020.111421.1190

Keywords: Uncertainty Analysis, Injection parameters, Spray Parameters, Injector, Injector plate, PDA.

1 Introduction

The evaluation of the uncertainty associated with a result is an essential part of quantitative analysis. Without knowledge of the measurement uncertainty, the statement of analytical and experimental results cannot be considered complete. The uncertainty arises from a variety of sources, and these can be categorized in different ways. The sources of uncertainty from analyses are well studied, but less focus has been upon uncertainty associated with a result. The approach to uncertainty estimation requires the identification of the possible sources of uncertainty for a procedure, followed by the evaluation of their magnitude. In this paper, a Liquid Fuel Micromotor is used as a case study to derive respective uncertainties. The function of the (LFM) engines is very depended on injection characteristics that are produced by injectors [1]. The method of fuel injection into the combustion chambers is very important

* Corresponding Author, Assistance Prof. of Aerospace Engineering, Aerospace Research Institute (Ministry of Science, Research and Technology), Tehran, Iran m.nadjafi@ari.ac.ir

† Associate Professor of Aerospace Engineering, Aerospace Research Institute (Ministry of Science, Research and Technology), Tehran, Iran farsi@ari.ac.ir

‡ Professor of Mechanical Engineering, Tarbiat Modares University (TMU), Tehran, Iran fommi@modares.ac.ir

Receive : 2019/07/17 Accepted : 2020/03/08

[2]. Because of, the complexity and unknowing of the spray atomization [3]. Most of the researches have been done for experimental in this case. This process is very obscurant and its mechanism is not so clear, because some of the droplets are break-up and joint again [4]. Therefore, the droplets with different sizes produce in this system that they are depended on the initial pressure and temperature of the interior of the combustion and evaporating the droplets too [5]. The factors affecting uncertainty in injection parameters assessment are of various types and arise from different sources. Oberkampf et al. [6] and Helton [7] referred uncertainties into two broad categories namely, aleatory or stochastic and subjective or epistemic uncertainty. Stochastic uncertainty is due to the randomness that is heterogeneity or diversity in a population of some type [8, 9]; For example, the frequency of failure may not be the same for all equipment [10]. Stochastic uncertainty refers to the different failure frequency values for different equipment [11]. In this case, the frequency distribution helps to reflect the difference between equipment and to segregate the equipment population into homogeneous smaller groups. The second type of uncertainty (subjective uncertainty) is mainly due to the lack of knowledge, measurement error, vagueness, ambiguity, under-specificity, indeterminacy, and subjective judgment [12]; The stochastic uncertainty is irreducible, as it is the inherent nature of the system under study [13]. The subjective uncertainty cannot be reduced due to inherent limits on the human capacity to process information, but to account for this uncertainty fuzzy set theory is used. Vose divided the total uncertainty into variability and uncertainty [14]. He proposed a term verity (the combined term for variability and uncertainty) to represent the total uncertainty [15]. In the uncertainty analysis literature, little attention has been paid by researchers for the assessment of the accuracy of experimentally observed data. In this regard, an example showing an uncertainty assessment for a model scale towing tank propulsion test [16] following the ITTC procedures [17]. As an example, the model uncertainty in the conceptual design of a monopropellant blow down hydrazine propulsion system is investigated [18]. However, the true values of measured variables are seldom (if ever) known and experiments inherently have errors, e.g., due to instrumentation, data acquisition and reduction limitations, and facility and environmental effects [19]. For these reasons, determination of truth requires estimates for experimental errors, which are referred to as uncertainties [19]. Uncertainty assessment of a model scale LFM injection test is done by means of AIAA-S-071-1995 Standard [20] that is one of the most applicable methods for experimental uncertainty assessment [21]. We will not discuss the computational formulas for this method; we assume that the readers are familiar with these methodologies. The bias limits (B) and precision limits (P) and total uncertainties (U) for single and multiple runs have been estimated for the droplet velocity (V_{inj}), droplet diameter (D_{mean} or D_{SMD}), spray penetration length (S) and spray angle (φ)[22], [23]. Estimating the uncertainty of an experimental result is an essential part of quantitative analysis. The approach to uncertainty estimation requires the identification of the possible sources of uncertainty for a procedure, followed by the evaluation of their magnitude. This paper addresses this topic of model uncertainty via probabilistic methods. The purpose of the procedure is to provide a block diagram Figure 2) for the injection test in a model scale LFM that including individual measurement systems, measurement of individual variables, data reduction, and experimental results. The remainder of the paper is organized as follows: Section 2 describes the accessories and facilities that are used in the lab. Section 3 presents the analysis of uncertainty for injection tests that contains Bias and Precision limits of components and laboratory conditions, and the effect of each parameter on the measured uncertainty. Section 4 depicts the results that represent the amount of total uncertainty by considering all entries that are affected in measurement. The last section presents the conclusions and future works.

2 Accessories of laboratories models

The laboratories models that are used in this investigation include injector, injector plates, and PDA, which are shown below. Note that, in this test, the liquid fuel is freshwater and the type of injectors that are used is the centrifugal injector bipod blending, and the arrangement of injectors on the injector plate has scheme of the circular injector plate (swirled atomizer). Finally, The PDA laboratory is used for measuring the velocity and diameters of droplets that are sprayed. All of the accessories of the model scale LFM are shown in Figure (1) on the collection mechanism.

3 Uncertainty Analysis for Injection Test

This procedure [24] provides an example showing an uncertainty assessment for a model scale LFM injection test. The bias limits (B) and precision limits (P) and total uncertainties for single and multiple runs have been estimated for the droplet velocity (V_{inj}), droplet diameter (D_{mean} *or* D_{SMD}), spray penetration length (***S***) and spray angle (φ) at model scale at one Reynolds number. In order to achieve reliable precision limits, it is recommended that 5 sets of tests in 4 point from the vertex of an injector in each set are performed giving in total 20 test points. In this example, the recommended sequence was followed [17].
Extrapolation to full scale has not been considered in this test. Although it might lead to significant sources of error and uncertainty, it is not essential for the present purpose of demonstrating the methodology. When performing an uncertainty analysis for a real case, the details need to be adapted according to the equipment used and procedures followed in each respective facility.

3.1 Test Design

By measuring the difference of injection pressure and chamber pressure (ΔP), injection mass flow ($\dot{m}$), nominal injector nozzle hole diameter (D), sac hole diameter (D_S), length of nozzle hole (L), and by measuring or using reference values of liquid properties (ρ, μ, σ) and water temperature parameters [measuring parameters], the spray penetration length (***S***), droplet velocity (V_{inj}), droplet diameter (D_{mean} *or* D_{SMD}) and spray angle (φ) [calculating parameters] can be calculated.

(a) Centrifugal injector (right to left: external injector, cap, internal injector and brazed injector)

(b) Phase Doppler Analyzer Measuring Device

(c) Exterior and Interior view of flat circular injector plate

Figure 1 Accessories of laboratory model: (a) Centrifugal Injector; (b) PDA; (c) Injector Plate

The spray penetration length (S), droplet velocity (V_{inj}), droplet diameter (D_{SMD}) and spray angle (φ) by use of measuring parameters can be defined as:
The time-dependent of the spray penetration length ***S*** can be obtained by Eq. (1) [4]:

$$S = 0.39\left(\frac{2\Delta P}{\rho_l}\right)^{1/2} \times t \tag{1}$$

Where ΔP is the difference between injection pressure and chamber pressure, ρ_l is the nominal mass density of freshwater in the tank set to $\rho_l = 1000$ kg/m^3, and ***t*** is the time from the beginning of injection ($t=0$) and ends at the moment the liquid jet emerging from the nozzle hole begins to disintegrate ($t=t_{break}$). The spray cone angle is another characteristic parameter of a full-cone spray that has the following relation:

$$\varphi = 83.5\left(\frac{L}{D}\right)^{-0.22} \times \left(\frac{D}{D_S}\right)^{0.15} \times \left(\frac{\rho_g}{\rho_l}\right)^{0.26} \tag{2}$$

where φ is the spray cone angle in [deg], D_S is the sac hole diameter in [m], and L is the length of the nozzle hole in [m], and ρ_g, ρ_l are liquid and gas (in this test, gas is the standard sea-level air) densities in [kg/m^3].

The Sauter Mean Diameter (SMD) of an injector can be expressed by the semi-empirical relation:

$$SMD = 2.25 \times \sigma^{1/4} \times \mu_l^{1/4} \times \dot{m}^{1/4} \times \Delta P^{-0.5} \times \rho_g^{-0.25} \tag{3}$$

Where $\dot{m}$ is the injection mass flow, and μ, σ are the water properties, and ρ_g is the air density of standard laboratory condition.

Droplet injection velocities are expressed as:

$$V_{inj}(t) = \frac{\dot{m}_{inj}(t)}{A_{hole} \times \rho_l} = \sqrt{\frac{2\Delta P_{inj}}{\rho_l}} \tag{4}$$

Where $A_{hole}=\pi.D^2/4$ is the cross-sectional area of the injector nozzle hole, and the ρ_l is the liquid density, and $\dot{m}_{inj}(t)$ is the fuel (water) mass flow rate (measurement).

The injection test requires both Cold-test and PDA test results. These tests have bias and precision errors, which may affect not only the uncertainty in scaling to liquid fuel motor injection prediction but also uncertainty in the injection process test. As these four tests were accepted as a minimum set of required tests for the determination of the liquid fuel motor injection, the effects of bias and precision errors of both Cold-test and PDA tests on injection test, bias errors were taken into account to predict the uncertainty in the droplet velocity (V_{inj}), droplet diameter (D_{SMD}), spray penetration length (S) and spray angle (φ).

3.2 Measurement System and Procedure

Measurement systems consist of the instrumentation, the procedures for data acquisition and reduction, and the operational environment, e.g., laboratory, large-scale specialized facility, and in situ. The methodology for estimating the uncertainties in measurements and in the experimental results calculated from them must be structured to combine statistical and engineering concepts. This must be done in a manner that can be systematically applied to each step in the data uncertainty assessment determination. Figure 2) shows a block diagram for the injection test in a model scale LFM that including individual measurement systems, measurement of individual variables, data reduction, and experimental results.

As shown, the source of effective parameters in spraying and injection process (Bias Sources) is depicted as individual measurement systems, and their respective parameters are categorized by measurement of individual variables, data reduction consists of respective relations and formula, and finally, the experimental results block to represent the required estimating parameters (Bias limits and Precision limits in order to estimate the total uncertainty value).

In **Section 3.3.1** the bias limits contributing to the total uncertainty will be estimated for individual measurement systems: Injector Geometry, Injector Mass-Flow, PDA System, Spray Penetration Length, Droplet Diameter, Droplet Velocity, Differential Pressure, Spray Angle, and Temperature/ Density/ Viscosity. The elementary bias limits are for each measurement system estimated for the categories: calibration, data acquisition, data reduction and conceptual bias [25].
The bias limits are then, using the data reduction Eqs. (1)-(4), reduced in to B_S, B_φ, B_{SMD} and B_V respectively.
The precision limits for the Spray Penetration Length (P_S), Spray Angle (P_φ) Droplet Diameter (P_{SMD}) and Droplet Velocity (P_V), in LFM model scale, are estimated by an end-to-end method for multiple tests (M) and a single run (S).

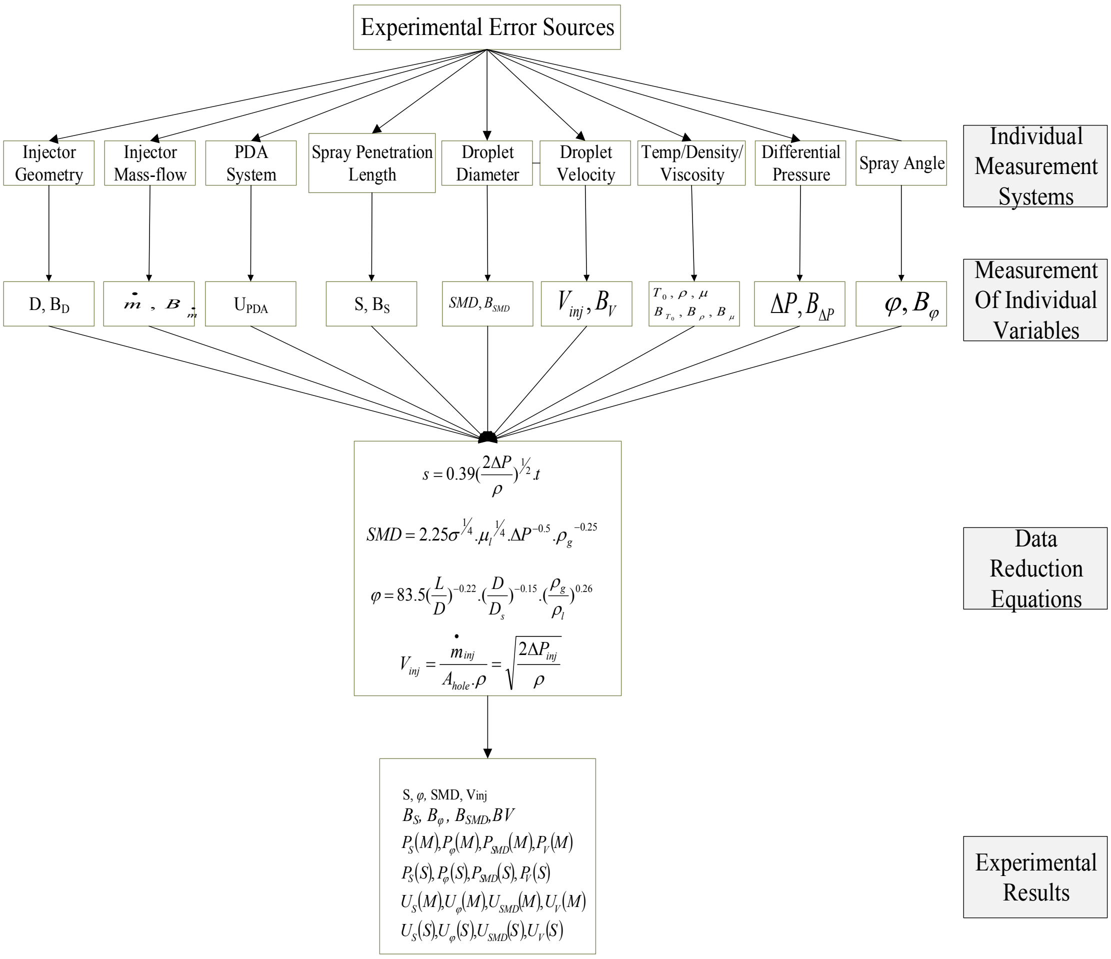

Figure 2 Block Diagram of Injection Test Procedure

3.3 Uncertainty Analysis

The total uncertainty (U) for the LFM injection coefficients are given by the root sum square of the uncertainties of the total bias (B) (Bias is a systematic error result from an estimation process that does not give accurate results on average) and precision (P) (Precision is a description of random errors) limits:

$$(U)^2=(B)^2+(P)^2 \tag{5}$$

The bias limits for Eqs. (1)-(4) are:

$$(B_S)^2=\left(\frac{\partial S}{\partial \Delta P}B_{\Delta P}\right)^2+\left(\frac{\partial S}{\partial \rho_l}B_{\rho_l}\right)^2+\left(\frac{\partial S}{\partial t}B_t\right)^2 \tag{6}$$

$$(B_\varphi)^2=\left(\frac{\partial \varphi}{\partial L}B_L\right)^2+\left(\frac{\partial \varphi}{\partial D}B_D\right)^2+\left(\frac{\partial \varphi}{\partial D_S}B_{D_S}\right)^2+\left(\frac{\partial \varphi}{\partial \rho_l}B_{\rho_l}\right)^2+\left(\frac{\partial \varphi}{\partial \rho_g}B_{\rho_g}\right)^2 \tag{7}$$

$$(B_{SMD})^2=\left(\frac{\partial SMD}{\partial \Delta P}B_{\Delta P}\right)^2+\left(\frac{\partial SMD}{\partial \rho_g}B_{\rho_g}\right)^2+\left(\frac{\partial SMD}{\partial \dot{m}}B_{\dot{m}}\right)^2+\left(\frac{\partial SMD}{\partial \sigma}B_\sigma\right)^2+\left(\frac{\partial SMD}{\partial \mu_l}B_{\mu_l}\right)^2 \tag{8}$$

$$(B_V)^2=\left(\frac{\partial V}{\partial \Delta P}B_{\Delta P}\right)^2+\left(\frac{\partial V}{\partial \rho}B_\rho\right)^2=\left(\frac{\partial V}{\partial \dot{m}}B_{\dot{m}}\right)^2+\left(\frac{\partial V}{\partial A}B_A\right)^2+\left(\frac{\partial V}{\partial \rho_l}B_{\rho_l}\right)^2 \tag{9}$$

The precision limits will be determined for the injection coefficients by an end-to-end method where all the precision errors for Injector Geometry, Injector Mass-Flow, PDA System, Spray Penetration Length, Droplet Diameter, Droplet Velocity, Differential Pressure, Spray Angle, and Temperature/ Density/ Viscosity are included. The precision limits for a single run (S) and for the mean value of multiple tests (M) are determined. The precision limit must be determined for single or multiple runs in order to include random errors such as model misalignment, trim, etc. If it is not possible to perform repeated tests the experimenter must estimate a value for the precision error using the best information available at that time. The precision limit for multiple tests is calculated according to:

$$P(M)=\frac{K\times SD_{ev}}{\sqrt{M}} \tag{10}$$

Where M = number of runs for which the precision limit is to be established, SDev is the standard deviation established by multiple runs and K=2 according to the methodology.

Also, the precision limit for a single run can be calculated according to:

$$P(S)=K\times SD_{ev} \tag{11}$$

It is not precisely known that the uncertainty value for a single run is certainly greater than the uncertainty for the multiple runs. Because the uncertainty amount for a particular test might be greater or less than the mean uncertainty, this depends on the test conditions and the measurement accuracy at each stage.

3.3.1 Bias Limit

Under each group of bias errors (Injector Geometry, Injector Mass-Flow, Temperature/ Density/ Viscosity, PDA System, Spray Penetration Length, Droplet Diameter, Droplet Velocity, Differential Pressure and Spray Angle) the elementary error sources have been divided into the following categories: calibration; data acquisition; data reduction; and conceptual bias. The categories not applicable for each respective section have been left out. Table (3.1) shows some constants used in this paper.

3.3.1.1 Injector Geometry

The injector model is manufactured to be geometrically similar to the drawing or mathematical model describing the hull form. Even though the great effort is given to the task of building a model no model manufacturing process is perfect and therefore each model has an error in form and cross-sectional area. The influence of an error in hull form affects not only the wetted surface but also the measured values by an error in mass-flow, Droplet velocity and spray angle. For example, two hull forms injector, with the same length and diameter, give different spray angle, spray penetration length, mass-flow, and droplets velocity and diameter when injected from injector ports. This error in hull form geometry is very difficult to estimate, and will not be considered here. Only the bias errors in model length and diameter due to model manufacture error are taken into account.

a. Model Lengths

The bias error in model length due to manufacturing error in model geometry can be adopted from the model accuracy of ±0.25 mm as given by the manufacturer (Data acquisition). Hence, the bias error in model length will be B_L=0.5 mm.

Table 3.1 Constants

Properties	Definitions	Symbol	Value (Units)
Water & Air Lab. Properties	Temperature	T	15.8 (˚c)
	Water Density	ρ	1000 (kg/m^3)
	Gas/Air Density	ρ_g	1.225 (kg/m^3)
	Water Dynamic Viscosity	μ	0.00114 (kg/m.s)
	Water Surface Tension	σ	0.073357 (N/m)
Model Accessories Geometry	Injector Length	L	2 (cm)
	Injector Diameter	D	1.1 (mm)
	Injector Hole Area	A_{hole}	0.95 (mm^2)
Nominal Injection Properties	Differential Pressure	ΔP	8 (bar)
	Total Mass-flow	$\dot{m}$	2.7 (kg/s)
	Mean Diameter	D_{mean}	0.115 (mm)
	Mean Velocity	V_{mean}	10.442 (m/s)
	Spray Angle	φ	75 (deg)
	Spray Penetration Length	S	45 (mm)
	Sac hole diameter	D_S	69.06 (mm)

b. Model Diameter

The bias error in model diameter due to manufacturing error in model geometry (Data acquisition) can be adopted from the model accuracy of ±0.0025 mm as given by the manufacturer. Which will result in a model diameter bias error of B_D=0.005 mm. Hence, $A_{hole}=\pi.D^2/4$ is the cross-sectional area of the injector nozzle hole, then $B_A=2\times10^{-5}$ mm^2.

3.3.1.2 TEMPERATURE/DENSITY/VISCOSITY

A. *Temperature*

The thermometer used is calibrated by the manufacturer with a guaranteed accuracy of ±0.30 degrees within the interval +5 to +40 degrees. The bias limit associated with temperature measurement (Calibration) is B_{T0}=0.3 degrees corresponding to 1.899% of the nominal temperature in injection tests of 15.8 degrees.

B. *Density/Viscosity*

The bias errors in density/viscosity of freshwater and density of air are affected by bias errors in temperature measurement. Therefore, in accordance with S.I standard (Data acquisition) and variation of ±0.30 degrees' temperature effects, the bias error limits for density and viscosity of water and density of air will be:

$$B_{\rho} = \left|\frac{\partial \rho}{\partial T_0}\right| \times B_{T_0} = 0.1582 \times 0.3 = 0.0474\,(kg/m^3) \qquad (12)$$

The bias limit for density is thus B_ρ=0.0474 (kg/m^3) corresponding to 0.00474% of ρ=1000.

The bias error limits for the viscosity of water will be:

$$B_{\mu} = \left|\frac{\partial \mu}{\partial T_0}\right| \times B_{T_0} = 0.00003 \times 0.3 = 9\times10^{-6}\,(kg/ms) \qquad (13)$$

Hence the total bias limit associated with freshwater viscosity due to temperature measurement is $B_\mu=9\times10^{-6}$ (kg/m.s) corresponding to 0.789% of the dynamic viscosity.
The bias error limits for the density of air will be:

$$B_{\rho_g} = \left|\frac{\partial \rho_g}{\partial T_0}\right| \times B_{T_0} = 0.004 \times 0.3 = 0.0012\,(kg/m^3) \qquad (14)$$

The bias limit for air density is thus $B_{\rho g}$=0.0012 (kg/m^3) corresponding to 0.098% of ρ_g=1.225 (kg/m^3).

C. *Water surface tension*

The bias errors in surface-tension of water are affected by bias errors in temperature measurement. Therefore, in accordance with S.I standard (Data acquisition) and variation of ±0.30 degrees' temperature effects, the bias error limits for density and viscosity of water and density of air will be:

$$B_{\sigma} = \left|\frac{\partial \sigma}{\partial T_0}\right| \times B_{T_0} = 0.00014 \times 0.3 = 42\times10^{-6}\,(N/m) \qquad (15)$$

Hence the total bias limit associated with fresh water surface-tension due to temperature measurement is $B_\sigma=42\times10^{-6}$ (N/m) corresponding to 0.057% of the standard value.

3.3.1.3 PDA SYSTEM

The application of the Phase Doppler measurement technique is to provide improved drop sizing and liquid water content measurements [26]. This instrument has the possibility of counting errors of two main types: coincidence losses and dead time losses.

The magnitudes of counting errors were analyzed because these errors contribute to inaccurate liquid water content measurement. The PDA counting errors due to data transfer losses and coincidence losses were analyzed for data input rates from 20 samples/ second to 60,000 samples/second. With direct memory access enabled, data transfer losses are less than 3 percent (such as $B_{PDA(t)}$=0.03). And the magnitude of the coincidence loss can be determined and is less than 5 percent (Max=5%) loss (such as $B_{PDA(c)}$ =0.05). Hence the total bias limit associated with an integrated PDA system due to bias errors for data transfer losses and coincidence loss can be calculated according to:

$$B_{PDA} = \sqrt{B_{PDA(t)}^{2} + B_{PDA(c)}^{2}} = \sqrt{(0.03)^2 + (0.05)^2} = 0.0583 \tag{16}$$

The total bias limit in PDA system is B_{PDA}=0.0583.

3.3.1.4 Injector Mass-Flow

Mass-flow that injected from each injector is calculated according to the following Eq. (17):

$$\dot{m}_{inj} = \rho \times V_{inj} \times A_{hole} \tag{17}$$

Bias errors in mass flow calculation may be traced back to errors in model diameter, fuel (water) density and injection velocity. Bias limit associated with $\dot{m}_{inj}$ can be a found as:

$$(B_{\dot{m}})^2 = \left(\frac{\partial \dot{m}}{\partial V} B_V\right)^2 + \left(\frac{\partial \dot{m}}{\partial A} B_A\right)^2 + \left(\frac{\partial \dot{m}}{\partial \rho} B_\rho\right)^2 \tag{18}$$

Partial derivatives of Eq. (18) by model cross-sectional area, fuel density and injection velocity are:

$$\begin{aligned}
\frac{\partial \dot{m}}{\partial \rho} &= V_{mean} \times A_{hole} = 10.442 \times 0.95 \times 10^{-6} = 9.923 \times 10^{-6} \left(m^3 / s\right) \\
\frac{\partial \dot{m}}{\partial A} &= V_{mean} \times \rho = 10.442 \times 1000 = 10442 \left(kg / m^2 s\right) \\
\frac{\partial \dot{m}}{\partial V} &= \rho \times A_{hole} = 1000 \times 0.95 \times 10^{-6} = 9.5 \times 10^{-4} \left(kg / m\right)
\end{aligned} \tag{19}$$

The total bias limit in injector mass-flow is

$$(B_{\dot{m}})^2 = \left(9.5 \times 10^{-4} \times 0.6\right)^2 + \left(10442 \times 2 \times 10^{-5}\right)^2 + \left(9.923 \times 10^{-6} \times 0.0474\right)^2 = 0.043615 \left(kg / s\right) \tag{20}$$

Hence the bias limit for mass-flow is corresponding to 7.7% of the nominal value.

3.3.1.5 Differential Pressure

The pressure indicator used is calibrated by the manufacturer with a guaranteed accuracy of ±2 mill bar within the interval +0.0 to +20 bars. The bias limit associated with differential pressure (Calibration) is $B_{\Delta P}$=0.004 bars corresponding to 0.05% of the nominal differential pressure behind the injectors in injection tests.

3.3.1.6 TOTAL BIAS LIMIT IN S.P.L

The total bias limit on the time-dependent of the spray penetration length ***S*** can be calculated according to Eq. (1) and Eq. (6). In Eq. (21), ***t*** is the time from the beginning of injection (***t****=0*) and ends at the moment the liquid jet emerging from the nozzle hole begins to disintegrate ($t=t_{break}$). This time is sensed by means of 8-Mpixel camera by tracking of a droplet emerging from injector nozzle hole to disintegrate and becoming vapor. Using the nominal value of *t*=0.01(sec), the total bias limit associated with the *S* is calculated based on Eq. (1) and Eq. (6). So the Partial derivatives of Eq. (6) by ΔP, *t,* and *ρ* will be:

$$\begin{aligned}
\frac{\partial S}{\partial \Delta P} &= 0.39(2\rho\Delta P)^{-1/2}.t = 0.308\times10^{-4}(m/N)\\
\frac{\partial S}{\partial \rho} &= -0.39\left(\frac{\Delta P}{2\rho^3}\right)^{1/2}.t = 0.247\times10^{-6}(m^4/kg)\\
\frac{\partial S}{\partial t} &= 0.39\left(\frac{2\Delta P}{\rho}\right)^{1/2} = 0.0493\,(m/s)
\end{aligned} \tag{21}$$

The camera module is factory calibrated and its rated accuracy is 1.02×10^{-5} (sec) on every update giving $B_t=1.02\times10^{-5}$ seconds. By use of Eq. (6) can be written:

$$\begin{aligned}
&(B_S)^2 = (0.308\times10^{-4}\times0.004)^2 +\\
&(0.247\times10^{-6}\times0.0474)^2 + (0.0493\times1.02\times10^{-5})^2.\\
&\Rightarrow (B_S)^2 = 0.526\times10^{-12}(m)
\end{aligned} \tag{22}$$

Hence the total bias limit associated with spray penetration length is $B_S=0.726\times10^{-3}$ (mm) corresponding to 0.0016% of the nominal value.

3.3.1.7 TOTAL BIAS LIMIT IN SPRAY ANGLE

The total bias limit on the spray angle ***φ*** can be calculated according to Eq. (2) and Eq. (7). Hence, the partial derivatives of Eq. (7) could be:

$$\begin{aligned}
\frac{\partial\varphi}{\partial L} &= \frac{-18.37\left(\frac{D}{D_S}\right)^{0.15}\times\left(\frac{\rho_g}{\rho_l}\right)^{0.26}}{D\times\left(\frac{L}{D}\right)^{1.22}} = -0.0456(\deg/m)\\
\frac{\partial\varphi}{\partial D} &= \frac{12.525\left(\frac{\rho_g}{\rho_l}\right)^{0.26}}{D_S\times\left(\frac{D}{D_S}\right)^{0.85}\times\left(\frac{L}{D}\right)^{0.22}} + \frac{18.37\left(\frac{D}{D_S}\right)^{0.15}\times L\left(\frac{\rho_g}{\rho_l}\right)^{0.26}}{D^2\times\left(\frac{L}{D}\right)^{1.22}} = 19.49(\deg/m)\\
\frac{\partial\varphi}{\partial D_S} &= \frac{-12.525\left(\frac{\rho_g}{\rho_l}\right)^{0.26}\times D}{D_S^2\times\left(\frac{D}{D_S}\right)^{0.85}\times\left(\frac{L}{D}\right)^{0.22}} = -0.009\,(\deg/\ m)\\
\frac{\partial\varphi}{\partial\rho_l} &= \frac{-21.71\left(\frac{D}{D_S}\right)^{0.15}\times\rho_g}{\rho_l^2\times\left(\frac{L}{D}\right)^{0.22}\times\left(\frac{\rho_g}{\rho_l}\right)^{0.74}} = -0.001\,(m^2\deg/\ kg)\\
\frac{\partial\varphi}{\partial\rho_g} &= \frac{21.71\left(\frac{D}{D_S}\right)^{0.15}}{\left(\frac{L}{D}\right)^{0.22}\times\left(\frac{\rho_g}{\rho_l}\right)^{0.74}\times\rho_l} = 0.88\,(m^2\deg/\ kg)
\end{aligned} \tag{23}$$

The total bias limit in spray angle is:

$$(B_{\varphi})^2 = (0.0456 \times 0.5)^2 + (19.49 \times 0.005)^2 + (0.009 \times 0.5)^2 + (0.001 \times 0.0474)^2 + (0.88 \times 0.0012)^2 \Rightarrow (B_{\varphi})^2 = 0.01(\deg) \tag{24}$$

The total bias limit associated with spray angle is B_{φ}=0.1 (deg) corresponding to 0.133% of the nominal value in Table (3.1).

3.3.1.8 *Total Bias Limit in Droplet Diameter*

The Sauter Mean Diameter (SMD) of an injector can be expressed by the semi-empirical relation [27] be calculated according to Eq. (3). Therefore, the total bias limit in this parameter can be obtained by Eq. (8). Partial derivatives of Eq. (8) will be:

$$\begin{aligned}
\frac{\partial SMD}{\partial \dot{m}} &= \frac{0.565\,\mu^{1/4} \times \sigma^{1/4}}{\rho_g^{0.25} \times \dot{m}^{3/4} \times \sqrt{\Delta P}} = 0.0087\,(ms/kg) \\
\frac{\partial SMD}{\partial \Delta P} &= \frac{-1.13\,\dot{m}^{1/4} \times \mu^{1/4} \times \sigma^{1/4}}{\Delta P^{3/2} \times \rho_g^{1/4}} = -0.0058\,(m/N) \\
\frac{\partial SMD}{\partial \sigma} &= \frac{0.565\,\dot{m}^{1/4} \times \mu^{1/4}}{\rho_g^{1/4} \times \sigma^{3/4} \times \sqrt{\Delta P}} = 0.32\,(m^2/N) \\
\frac{\partial SMD}{\partial \mu_l} &= \frac{0.565\,\dot{m}^{1/4} \times \mu^{1/4} \times \sigma^{1/4}}{\rho_g^{1/4} \times \mu^{3/4} \times \sqrt{\Delta P}} = 0.167\,(m^2 s/kg) \\
\frac{\partial SMD}{\partial \rho_g} &= \frac{-0.565\,\dot{m}^{1/4} \times \mu^{1/4} \times \sigma^{1/4}}{\rho_g^{5/4} \times \sqrt{\Delta P}} = -0.017\,(m^4/kg)
\end{aligned} \tag{25}$$

The total bias limit in droplet diameter is:

$$(B_{SMD})^2 = (-0.0058 \times 0.004)^2 + (-0.017 \times 0.0012)^2 + (0.0087 \times 0.208)^2 + (0.32 \times 42 \times 10^{-6})^2 + (0.167 \times 9 \times 10^{-6})^2 \Rightarrow (B_{SMD})^2 = 0.33 \times 10^{-5}(m) \tag{26}$$

The total bias limit associated with droplet Sauter Mean Diameter is B_{SMD}=0.00181 (mm) corresponding to 0.163% of the nominal value in Table (3.1).

3.3.1.9 *Total Bias Limit in Droplet Velocity*

Droplet velocity is expressed in the form as calculated according to Eq. (4). Therefore, the total bias limit in Droplet velocity can be calculated according to Eq. (9). Hence, the partial derivatives of Eq. (9) are as follows:

$$\begin{aligned}
\frac{\partial V}{\partial \dot{m}} &= \frac{1}{A_{hole} \times \rho_l} = \frac{1}{0.95 \times 10^{-3} \times 1000} = 1.052(m/kg) \\
\frac{\partial V}{\partial A} &= \frac{-\dot{m}}{A_{hole}^2 \times \rho_l} = \frac{-2.7}{(0.95 \times 10^{-3})^2 \times 1000} = -2991.7(1/ms) \\
\frac{\partial V}{\partial \rho_l} &= \frac{-\dot{m}}{A_{hole} \times \rho_l^2} = \frac{-2.7}{0.95 \times 10^{-3} \times (1000)^2} = -0.003(m^4/kgs)
\end{aligned} \tag{27}$$

The total bias limit in droplet velocity is:

$$(B_V)^2 = (1.052 \times 0.208)^2 + (-2991.7 \times 2 \times 10^{-5})^2 + (-0.003 \times 0.0474)^2 \Rightarrow (B_V)^2 = 0.0515(m/s) \tag{28}$$

The total bias limit associated with droplet velocity is B_V=0.227 (m/s) corresponding to 2.17% of the nominal relative value in Table (3.1).

3.3.2 Precision Limit

In order to establish the precision limits, the standard deviation for a number of tests, with the model removed and reinstalled between each set of measurements, must be determined. In this example, 5 sets of testing (A-E) of tests in 4 point from the vertex of an injector in each set have been performed giving in total 20 test points. This is a suitable way to include random errors in the set-up such as model misalignment, trim, etc. When performing an injection test at the different points from the injector nozzle hole, small deviations will occur. When a run is performed, the Spray Penetration Length, Droplet Diameter, Droplet Velocity, and Spray Angle are normally corrected to the nominal ΔP under the assumption that the spray penetration length (S), droplet velocity (V_{inj}), droplet diameter (D_{mean} *or* D_{SMD}) and spray angle (φ) are constant. When the measurements are repeated it is likely that the measured quantities will be taken at slightly different pressures for the different runs, and with different water temperatures between the different set of tests. In this case, no corrections have to be made for these deviations. The values used for the extrapolation of model test results are the Spray Penetration Length, Droplet Diameter, Droplet Velocity, and Spray Angle. These values are assumed to be constant for small deviations (as described above) and for small deviations in differential pressure and should therefore not be corrected. A correction for the difference in temperature between the different sets of tests is also not carried out because the temperature of the testing perimeter hasn't significant changes. In Table (3.2) the spray penetration length (S), droplet velocity (V_{inj}), droplet diameter (D_{SMD}) and spray angle (φ) given have been calculated based on measured quantities. The values below are valid for a model differential pressure of ($P_{oxidizer}$=6bar and P_{fuel}=8bar). On the other hand, the mean values, standard deviation (*SDev*), precision limits for single runs Eq. (11), and precision limits for multiple runs Eq. (10) have been calculated. The corresponding percentage values have also been given within brackets. The mean value over 20 runs for spray penetration length as $\overline{S}$=4.5 (cm) as shown in Table (3.2). The precision limit for the mean value of 20 runs is calculated as:

$$P_S(M) = \frac{K \times SDev_S}{\sqrt{M}} = \frac{2 \times 0.002}{\sqrt{20}} = 0.000895\ (m) \tag{29}$$

Corresponding to 1.99% of ***S***. for a single run the precision limit is calculated as:

$$P_S(S) = K \times SDev_S = 2 \times 0.002 = 0.004 \tag{30}$$

Corresponding to 8.89% of ***S***.

The mean value over 20 runs for spray angle as $\overline{\varphi}$=75 (deg) as shown in Table (3.2). The precision limit for the mean value of 20 runs is calculated as:

$$P_\varphi(M) = \frac{K \times SDev_\varphi}{\sqrt{M}} = \frac{2 \times 2}{\sqrt{20}} = 0.895(\deg) \tag{31}$$

Corresponding to 1.2% of $\boldsymbol{\varphi}$. for a single run the precision limit is calculated as:

$$P_S(S) = K \times SDev_S = 2 \times 2 = 4(\deg) \quad (32)$$

Corresponding to 5.34% of $\boldsymbol{\varphi}$.
The mean value over 20 runs for droplet diameter as $\overline{D}_{mean}$ =0.115 (mm) as shown in Table (3.2) the precision limit for the mean value of 20 runs is calculated as:

$$P_{SMD}(M) = \frac{K \times SDev_{SMD}}{\sqrt{M}} = \frac{2 \times 0.004}{\sqrt{20}} = 0.00179\ (mm) \quad (33)$$

Corresponding to 1.56% of $\boldsymbol{D_{mean}}$. For a single run the precision limit is calculated as:

$$P_S(S) = K \times SDev_S = 2 \times 0.004 = 0.008\ (mm) \quad (34)$$

Corresponding to 6.96% of $\boldsymbol{D_{mean}}$.
Finally, the mean value over 20 runs for droplet velocity as $\overline{V}_{mean}$ =10.442 (m/s) as shown in Table (3.2). The precision limit for the mean value of 20 runs is calculated as:

$$P_V(M) = \frac{K \times SDev_V}{\sqrt{M}} = \frac{2 \times 0.5}{\sqrt{20}} = 0.22\ (m/s) \quad (35)$$

Corresponding to 2.14% of $\boldsymbol{V_{mean}}$. For a single run the precision limit is calculated as:

$$P_S(S) = K \times SDev_S = 2 \times 0.5 = 1.0(m/s) \quad (36)$$

Corresponding to 9.58% of V_{mean}.

4 Total Uncertainties for Injection Test

By combining the precision limits for multiple and single tests with the bias limits, the total uncertainty can be calculated according to Eq. (5). The Total uncertainty of spray penetration length (S) for the multiple runs by the mean value of 20 runs will then be

$$\begin{aligned} U_S &= \sqrt{B_S^2 + P_S(M)^2} = \sqrt{\left(0.726 \times 10^{-3}\right)^2 + (0.000895)^2} \\ \Rightarrow U_S(M) &= \sqrt{1.328 \times 10^{-6}} = 0.00115\ (m) \end{aligned} \quad (37)$$

This is corresponding to 2.56% of S.
Correspondingly the total uncertainty for a single run can be calculated as:

$$\begin{aligned} U_S &= \sqrt{B_S^2 + P_S(S)^2} = \sqrt{\left(0.726 \times 10^{-3}\right)^2 + (0.004)^2} \\ \Rightarrow U_S(S) &= \sqrt{16.5 \times 10^{-6}} = 0.00401\ (m) \end{aligned} \quad (38)$$

The total uncertainty of spray penetration length is 0.00401 which is 9.03% of S.

The total uncertainty of spray angle (φ) for the mean value of 20 runs will then be

$$U_\varphi(M) = \sqrt{B_\varphi^2 + P_\varphi(M)^2} = \sqrt{(0.1)^2 + (0.895)^2} = 0.9(\deg) \quad (39)$$

This is corresponding to 1.2% of φ.
Correspondingly the total uncertainty for a single run can be calculated as

$$U_\varphi(S) = \sqrt{B_\varphi^2 + P_\varphi(S)^2} = \sqrt{(0.1)^2 + (4)^2} = 4.001(\deg) \quad (40)$$

This is 5.33% of φ.
The total uncertainty of droplet diameter (D_{SMD}) for the mean value of 20 runs will then be

$$U_{SMD} = \sqrt{B_{SMD}^2 + P_{SMD}(M)^2} = \sqrt{(0.00181)^2 + (0.00179)^2}$$
$$\Rightarrow U_{SMD}(M) = \sqrt{6.48 \times 10^{-6}} = 0.0026(m) \quad (41)$$

This is corresponding to 2.26% of D_{SMD} or D_{mean}.
Correspondingly the total uncertainty for a single run can be calculated as

$$U_{SMD} = \sqrt{B_{SMD}^2 + P_{SMD}(S)^2} = \sqrt{(0.00181)^2 + (0.008)^2}$$
$$\Rightarrow U_{SMD}(S) = \sqrt{67.27 \times 10^{-6}} = 0.0082(m) \quad (42)$$

This is 7.13% of D_{SMD} or D_{mean}.
The total uncertainty of droplet velocity (V_{inj}) for the mean value of 20 runs will then be

$$U_V = \sqrt{B_V^2 + P_V(M)^2} = \sqrt{(0.227)^2 + (0.22)^2}$$
$$\Rightarrow U_V(M) = \sqrt{0.0992} = 0.316(m/s) \quad (43)$$

This is corresponding to 3.03% of V_{inj}.
Correspondingly the total uncertainty for a single run can be calculated as

$$U_V = \sqrt{B_V^2 + P_V(S)^2} = \sqrt{(0.227)^2 + (1.0)^2}$$
$$\Rightarrow U_V(S) = \sqrt{1.052} = 1.025(m/s) \quad (44)$$

This is 9.82% of V_{inj}.

Table 3.2 Mean values, standard deviation and precision limits of S, V_{inj}, D_{SMD} and φ

Series/run	Injection factors based on measured values			
⇩	*S(mm)*	*φ(deg)*	V_{inj}*(m/s)*	D_{SMD}*(mm)*
A_1	45.3	73.5	10.73	0.113
A_2	45.1	74	10.00	0.115
A_3	45.15	75	11.10	0.1165
A_4	44.7	75.4	10.442	0.117
B_1	44.9	75.3	10.28	0.1090
B_2	44.85	76.5	11.15	0.114
B_3	45.14	73.0	10.08	0.115
B_4	45.20	73.8	12.00	0.1135
C_1	44.86	74.0	10.20	0.116
C_2	44.80	76.2	9.85	0.121
C_3	44.4	75	10.440	0.1155
C_4	43.9	74.6	9.58	0.118
D_1	46.10	74.7	11.45	0.115
D_2	45.0	76	10.39	0.1161
D_3	45.5	75.9	10.67	0.115
D_4	45.33	76.0	9.84	0.118
E_1	45	75	10.445	0.1145
E_2	45	74.1	12.03	0.112
E_3	44.67	75.0	11.06	0.1139
E_4	44.5	77.0	10.04	0.112
Mean	45	75	10.442	0.115
SDev	0.002	2	0.5	0.004
P(S)	0.004 [8.89%]	4.0 [5.34%]	1.0 [9.58%]	0.008 [6.96%]
P(M)	895×10^{-6} [1.99%]	0.895 [1.2%]	0.22 [2.14%]	0.00179 [1.56%]

As can be seen from the values above, the uncertainty will decrease if it is calculated for the mean value of 20 tests compared with the single run value. Expressed in relative numbers, the bias represents 63.13% and 18.1% of the total uncertainty for multiple tests and single run respectively for spray penetration length (S). For spray angle (φ) the bias represents 11.1% and 2.5% of the total uncertainty for multiple tests and a single run respectively.
Meanwhile, the bias represents 69.6% and 22.07% of the total uncertainty for multiple tests and a single run respectively for spray diameter (*SMD*). Also, the bias represents 71.84% and 22.15% of the total uncertainty for multiple tests and a single run respectively for spray velocity (V_{inj}). The bias and precision limits and the total uncertainties are summarized in Table (4.1). By comparing the bias and precision limits and the uncertainties, the relative contribution of each term can be calculated. This makes it possible to determine where an upgrade in the measurement system has the largest effect.

Uncertainty analysis results that are taken to spraying parameters show the high accuracy of multiple experimental test results (as calculated, 2.5%, 1.2%, 2.26%, and 3.03% total uncertainties are measured for Spray penetration length, Spray angle, Droplet mean diameter and Droplet velocity, respectively).

Table 4.1 Uncertainties in injection tests

Run(s)/ parameter	Total uncertainties		Percentage values
Multiple runs for S(*m*)	B_S (M)	0.726×10^{-3}	63.13% of U_S
	P_S(M)	0.895×10^{-3}	36.87% of U_S
	U_S(M)	0.00115	2.5% of S
Single run for S (*m*)	B_S (S)	0.726×10^{-3}	18.1% of U_S
	P_S(S)	0.004	81.9% of U_S
	U_S(S)	0.00401	9.03% of S
Multiple runs for φ(*deg*)	B_φ (M)	0.1	11.1% of U_φ
	P_φ(M)	0.895	88.9% of U_φ
	U_φ(M)	0.9	1.2% of φ
Single run for φ(*deg*)	B_φ (S)	0.1	2.5% of U_φ
	P_φ(S)	4	97.5% of U_φ
	U_φ(S)	4.001	5.33% of φ
Multiple runs for SMD(*m*)	B_{SMD} (M)	1.81×10^{-3}	69.6% of U_{SMD}
	P_{SMD}(M)	0.00179	30.4% U_{SMD}
	U_{SMD}(M)	0.0026	2.26% of SMD
Single run for SMD(*m*)	B_{SMD} (S)	1.81×10^{-3}	22.07% of U_{SMD}
	P_{SMD}(S)	0.008	77.9% of U_{SMD}
	U_{SMD}(S)	0.0082	7.13% of SMD
Multiple runs for V_{inj}(*m/s*)	B_V (M)	0.227	71.84% of U_V
	P_V(M)	0.22	28.16% of U_V
	U_V(M)	0.316	3.03% of V_{inj}
Single run for V_{inj}(*m/s*)	B_V (S)	0.227	22.15% of U_V
	P_V(S)	1.0	77.85% of U_V
	U_V(S)	1.025	9.82% of V_{inj}

5 Conclusion and Future Work

Estimation of uncertainties is one of complementary works for assessment of research results associated with the methods used for any process. Uncertainty estimation requires the identification of the possible sources of uncertainty for a procedure, followed by the evaluation of their magnitude. In the field of spraying in the injection process, its parameters (droplet's velocity, droplet's diameter, spray angle and spray penetration length) are the most important factors in combustion process that depends on some factors such as: The type of injector, injector arrangements in injector plate and the type of combustion chamber. The first aim of this paper is evaluation of the injection parameters from the viewpoint of macroscopic and microscopic in a manufactured model scale Liquid Fuel Micromotor (LFM) that are measured experimentally in Cold-Test and Phase Doppler Analyzer (PDA) laboratories, and then, Uncertainty Analysis (UA) methodologies for experimental uncertainty assessment are implemented to drive respective block diagram. The applied methodology for this case contains a block diagram that including individual measurement systems, measurement of individual variables, data reduction and experimental results for a model scale LFM injection tests. The sources of uncertainty associated with the techniques are presented, and where such data were available, quantitative estimates of their magnitude are given. Uncertainty analysis results that are taken to spraying parameters show the high accuracy of experimental test results (nominally, 2.5%, 1.2%, 2.26%, and 3.03% total uncertainties are measured for Spray penetration length, Spray angle, Droplet mean diameter and Droplet velocity, respectively). This framework is a comprehensive and complete technique that could be implemented and executed over any sets to analyze uncertainty value, with the difference that each set or case study has its respective parameters. In the future work, we want to extend this search to cover the uncertainty propagation in each step and over any parameter in order to exact evaluation of total uncertainty amount. Also, with the help of fuzzy set theory, the concept, interpretation, and importance of the uncertainty will be studied.

Acknowledgment

The authors gratefully acknowledge the devoting from precious professor his Excellency M. Ashjaei (professor of mechanical engineering, University of Tehran (UT)) for it is unsparing guidance in improving and accomplishing this research. Special thanks to Excellency Mr. Farajpour Eng. in improving this project. Also, Mr. M. Taheri that helps us in laboratory experiment operations.

References

[1] Sutton, G.P., and Biblarz, O., "*Rocket Propulsion Elements*", John Wiley & Sons, New York, (2016).

[2] Nadjafi, M., "Modeling and Experimental Investigation of Injection Process in Micromotor Combustion Chamber of Liquid Fuel Engines", M.S. Thesis, Tarbiat Modarres University, Tehran, Iran, Jun (2010).

[3] Giffen, E., and Muraszew, A., "*The Atomization of Liquid Fuel*", Chapman and Hall, London, (1953).

[4] Baumgarten, C., "*Mixture Formation in Internal Combustion Engines*", Springer Science & Business Media, Hannover, (2006).

[5] Mayer, W. O. H., and Branam, R., "Atomization Characteristic on the Surface of a Round Liquid Jet", Experiments in Fluid, ISSN 0723-4864, Vol. 36, No. 4, pp. 528-539, (2004).

[6] Oberkampf, W.L., Helton, J.C., Joslyn, C.A., Wojtkiewicz, S.F., and Ferson, S., "Challenge Problems: Uncertainty in System Response Given Uncertain Parameters", Reliability Engineering & System Safety, Vol. 85, No. 1, pp. 11-19, (2004).

[7] Helton, J.C., "Uncertainty and Sensitivity Analysis Techniques for use in Performance Assessment for Radioactive Waste Disposal", Reliability Engineering & System Safety, Vol. 42, No. 2, pp. 327-367, (1993).

[8] Frey, H.C., and Rubin, E.S., "Evaluation of Advanced Coal Gasification Combined-Cycle Systems under Uncertainty", Industrial & Engineering Chemistry Research, Vol. 31, No. 5, pp. 1299-1307, (1992).

[9] Siuta, D., Markowski A.S., and Mannan M.S., "Uncertainty Techniques in Liquefied Natural Gas (LNG) Dispersion Calculations", Journal of Loss Prevention in the Process Industries, Vol. 26, No. 3, pp. 418-426, (2013).

[10] Mousavi, S.S., and Behbahani, S., "Uncertainty Quantification with Hybrid Alpha-cut", Soft Computing, Vol. 23, No. 16, pp. 7321-7331, (2019).

[11] Arunraj, N., Mandal, S., and Maiti, J., "Modeling Uncertainty in Risk Assessment: An Integrated Approach with Fuzzy Set Theory and Monte Carlo Simulation", Accident Analysis & Prevention, Vol. 55, pp. 242-255, (2013).

[12] Helton, J.C., "Uncertainty and Sensitivity Analysis in the Presence of Stochastic and Subjective Uncertainty", Journal of Statistical Computation and Simulation, Vol. 57, No. 1, pp. 3-76, (1997).

[13] Van der Pas, J.W., Marchau, V.A., Walker, W.E., Van Wee, G.P., and Vlassenroot, S.H., "ISA Implementation and Uncertainty: A Literature Review and Expert Elicitation Study", Accident Analysis & Prevention, Vol. 48, pp. 83-96, (2012).

[14] Hart, A., Smith, G.C., Macarthur, R., and Rose, M., "Application of Uncertainty Analysis in Assessing Dietary Exposure", Toxicology Letters, Vol. 140, pp. 437-442, (2003).

[15] Smith, E., "*Uncertainty Analysis*", Wiley StatsRef: Statistics Reference Online, Wiley Online Library, John Wiley & Sons, (2014).

[16] ITTC, "Uncertainty Analysis, Example for Propulsion Test", 23rd ITTC-Recommended Procedures, ITTC 7.5-02-03-01.2, pp. 1-26, Venice, Italy, (2002).

[17] ITTC, "Uncertainty Assessment Methodology", ITTC Procedures for Uncertainty Analysis in EFD 7.5-02-01-01 Rev00, Venice, Italy, (2002).

[18] Thunnissen, D.P., "Uncertainty Classification for the Design and Development of Complex Systems", 3rd Annual Predictive Methods Conference, Newport Beach, California, (2003).

[19] Coleman, H.W., and Steele, W.G., "*Experimentation, Validation, and Uncertainty Analysis for Engineers*", John Wiley and Sons, 2nd Edition, Inc., New York, (2018).

[20] Standard, A., "AIAA Standard (1995) for Experimental Uncertainty Assessment Methodology", AIAA-S-071-1995, (1995).

[21] Stern, F., Muste, M., Beninati, M.L., and Eichinger, W.E., "Summary of Experimental Uncertainty Assessment Methodology with Example", IIHR Report, Iowa Institute of Hydraulic Research, the University of Iowa, (1999).

[22] Vassalo, P., and Ashgriz, N., "Effect of Flow Rate on the Spray Charactersitics of Impinging Water Jets", Journal of Propulsion and Power, Vol. 8, No. 5, pp. 980-986, (1992).

[23] Brink, J.S., "Reverse Kinematic Analysis and Uncertainty Analysis of the Space Shuttle AFT Propulsion System (APS) POD Lifting Fixture", Doctoral Dissertation, University of Florida, (2005).

[24] Frank, M.V., "Case Studies of Uncertainty Analysis in Reliability and Risk Assessment", Annual Reliability and Maintainability Symposium, Washington, DC, (1999).

[25] Kiedaisch, J., and Gravante, S., "Calibration of CFD Spray Model Parameters using Detailed Experimental Spray Characterization Data", ICLASS, 11th Triennial International Conference on Liquid Atomization and Spray Systems, Proceedings of a Meeting Held 26-30 July 2009, Vail, Colorado, USA, (2009).

[26] Reitz, R., and Bracco, F., "Mechanisms of Breakup of Round Liquid Jets", Encyclopedia of Fluid Mechanics, Vol. 3, pp. 233-249, Gulf Publishing Company, Houston, Texas, USA, (1986).

[27] Sarchami, A., Ashgriz, N., and Tran, H., "A Spray Model to Predict Droplet Size Distribution Produced by Wall Impingement Nozzle", in 38th Fluid Dynamics Conference and Exhibit, AIAA 2008-3837, https://doi.org/10.2514/6.2008-3837, Seattle, Washington, (2008).

Nomenclature and Abbreviations

A_{hole}	Injector Hole Area
B	Bias Limit= Systematic Error
D	Injector Nozzle Hole Diameter
D_{mean}	Droplet Mean Diameter
D_S	Sac Hole Diameter
K	Coefficient of Precision Limit
L	Length of Injector Nozzle
LFM	Liquid Fuel Micromotor
M	Multiple runs
P	Precision Limit= Random Error
PDA	Phase Doppler Analyzer
Sac	Injector Nozzle Hole

SMD	Sauter Mean Diameter
S	Single run
$\boldsymbol{S}$	Spray Penetration Length
T	Temperature
U	Uncertainty
UA	Uncertainty Analysis
V_{inj}	Droplet Velocity
Φ	Spray Angle
ΔP	Difference of Injection pressure and Chamber Pressure
$\dot{m}$	Injection Mass-Flow
ρ_l	Mass Density of Fresh Water
μ	Dynamic Viscosity of Fresh Water
σ	Water Surface Tension
ρ_g	Gas/Air Density
$B_{\boldsymbol{S}}$	Bias Limit for Spray Penetration Length
B_{φ}	Bias Limit for Spray Angle
B_{SMD}	Bias Limit for Droplet Mean Diameter
B_V	Bias Limit for Droplet Velocity
$P_{\boldsymbol{S}}$	Bias Limit for Spray Penetration Length
P_{φ}	Bias Limit for Spray Angle
P_{SMD}	Bias Limit for Droplet Mean Diameter
P_V	Bias Limit for Droplet Velocity
$P(M)$	Precision Limit for Multiple Runs
$P(S)$	Precision Limit for Single Run
$U(M)$	Total Uncertainty for Multiple Runs
$U(S)$	Total Uncertainty for Single Run